MLST

RESEARCH PAPER

Optimizing the hybridization chain reaction-fluorescence in situ hybridization (HCR-FISH) protocol for detection of microbes in sediments

Zeyu Jia[1] · Yijing Dong[2] · Heng Xu[2,3] · Fengping Wang[1,4]

Abstract

Fluorescence in situ hybridization (FISH) is a canonical tool commonly used in environmental microbiology research to visualize targeted cells. However, the problems of low signal intensity and false-positive signals impede its widespread application. Alternatively, the signal intensity can be amplified by incorporating Hybridization Chain Reaction (HCR) with FISH, while the specificity can be improved through protocol modification and proper counterstaining. Here we optimized the HCR-FISH protocol for studying microbes in environmental samples, particularly marine sediments. Firstly, five sets of HCR initiator/amplifier pairs were tested on the laboratory-cultured bacterium *Escherichia coli* and the archaeon *Methanococcoides methylutens*, and two sets displayed high hybridization efficiency and specificity. Secondly, we tried to find the best combination of sample pretreatment methods and HCR-FISH protocol for environmental sample analysis with the aim of producing less false positive signals. Various detachment methods, extraction methods and formulas of hybridization buffer were tested using sediment samples. Thirdly, an image processing method was developed to enhance the DAPI signal of microbial cells against that of abiotic particles, providing a reliable reference for FISH imaging. In summary, our optimized HCR-FISH protocol showed promise to serve as an addendum to traditional FISH for research on environmental microbes.

Keywords Fluorescence in situ hybridization · Hybridization chain reaction · HCR-FISH · Microbial detection · Sediment

Edited by Chengchao Chen.

✉ Heng Xu
Heng_Xu@sjtu.edu.cn

✉ Fengping Wang
fengpingw@sjtu.edu.cn

1   State Key Laboratory of Microbial Metabolism, Joint International Research Laboratory of Metabolic and Developmental Sciences, School of Life Sciences and Biotechnology, Shanghai Jiao Tong University, Shanghai 200240, China

2   School of Physics and Astronomy, Shanghai Jiao Tong University, Shanghai 200240, China

3   Institute of Natural Science, Shanghai Jiao Tong University, Shanghai 200240, China

4   School of Oceanography, Shanghai Jiao Tong University, Shanghai 200240, China

Introduction

Fluorescence in situ hybridization (FISH) is a widely used research tool in studying the environmental microbial community (Yamaguchi and Kubota 2017). By labelling 16S rRNA, FISH can phylogenetically distinguish targeted microbes at the single-cell level. The applications of FISH in environmental research include quantification of specific microbial populations (Baptista et al. 2014; Buongiorno et al. 2017), cell-level exploration of spatial structure of microbial communities (Orcutt and Meile 2008; Wilen et al. 2008), and providing an indication of cell location for other high-resolution imaging techniques such as Nanoscale secondary ion mass spectrometry (nanoSIMS), Bio-Orthogonal Non-Canonical Amino acid Tagging (BONCAT), and Raman microscopy (Chen et al. 2014; Hatzenpichler et al. 2016; Huang et al. 2007).

In order to observe microbes with epi-fluorescence microscopes, the fluorescence signal of the targeted cells must be intensive and specific. High signal intensity ensures that targeted cells can be distinguished from

background signals, and the high specificity ensures that untargeted cells and abiotic particles are not mis-recognized as targeted cells. The traditional FISH method usually works well on highly active microbes on both signal intensity and specificity (Wilen et al. 2008). However, microbial cells in sediment are typically less active and/ or smaller in size than *E. coli* (Amann and Fuchs 2008; Orphan et al. 2009), with inadequate amounts of rRNA for traditional FISH to create signals intense enough to distinguish cells from the background (Fazi et al. 2007). In addition to using fluorophores with higher efficiency, a variety of signal amplification methods have been tried and combined with FISH to explore the microbial communities in sediments (Amann et al. 1995). One method is to design multiple probes targeting different loci of the same rRNA, thus strengthening the signal of each rRNA (Morris et al. 2002). Another method is to deploy a multi-labeled polynucleotide probe, e.g., using RNA transcripts from PCR amplicons of 16S and 23S rRNA genes, with multiple fluorescently labeled uridine incorporated during transcription (Pernthaler et al. 2002). Other methods have been borrowed from sensor technology, of which the catalyzed reporter deposition FISH (CARD-FISH) is the most well-reported (Kubota 2013). This method requires a DNA probe labeled with horseradish peroxidase (HRP). This enzyme can induce the reaction of hydroperoxide, fluorescence-labeled tyramide, and intracellular aromatic compounds, leading to a deposition of tyramide on the target site. Although this method significantly increases the fluorescence signal, some issues have restricted its application on sediment samples (Kubota 2013): the large molecular weight (~ 40 kDa) of HRP prevents the entrance of the probe into the cells, thus extra permeabilization should be undertaken prior to the hybridization; H_2O_2 is necessary for inactivation of intracellular peroxidase to avoid a false-positive result, however, this may degrade the nucleic acid (Massie et al. 1972).

Hybridization chain reaction (HCR) is another signal amplification method (Dirks and Pierce 2004). It is a strand displacement amplification method, where the nicked double-helix nucleotide strand is produced without the use of enzyme and a change of temperature. For example, in DNA HCR process, the presence of the initiator oligonucleotide triggers a repeating hybridization of two species of DNA hairpins. By combining the initiator with different type of molecules, such as aptamer (Bao et al. 2020; Jia et al. 2018; Zhang et al. 2020), antibodies (Choi et al. 2011), DNA probes (Yamaguchi et al. 2015b), nanoparticles (Zeng et al. 2019; Zhang et al. 2012), etc., the long-chain double-stranded DNA (dsDNA) can specifically locate the target molecule. Since the DNA hairpins can incorporate the fluorophore (Huang et al. 2011), nanoparticles (Gao et al. 2017; Miao et al. 2015; Wu et al. 2018), electrochemical indicator (Hou et al. 2015), etc., the amplified signal can be detected by diverse kinds of instruments, such as spectrophotometers, electrodes and transmission electron microscopes (Bi et al. 2017).

Of the described methods, the combination of HCR with FISH for bio-imaging was first reported in 2010 (Choi et al. 2010). In HCR-FISH, the aforementioned initiators in the HCR system are concatenated to the probes of traditional FISH as initiator probes. Unlike the fluorescently labeled FISH probe, the initiator probes of HCR-FISH are not labeled. Two amplifier probes, A and B, are also required for HCR-FISH, each of which is fluorescently labeled and has a stable hairpin structure with free tails on their 5′ terminal. At the beginning, initiator probes hybridize with targeted intracellular RNA, leaving their initiator sequence unpaired (Fig. 1, process I). After the removal of excessive initiator probes, amplifier probes A and B can be added. The unpaired initiator sequence binds to the unpaired tail of probe A, linearizing the stem-loop structure (Fig. 1, process II). The released sequence on the stem-loop structure similarly binds to the unpaired tail
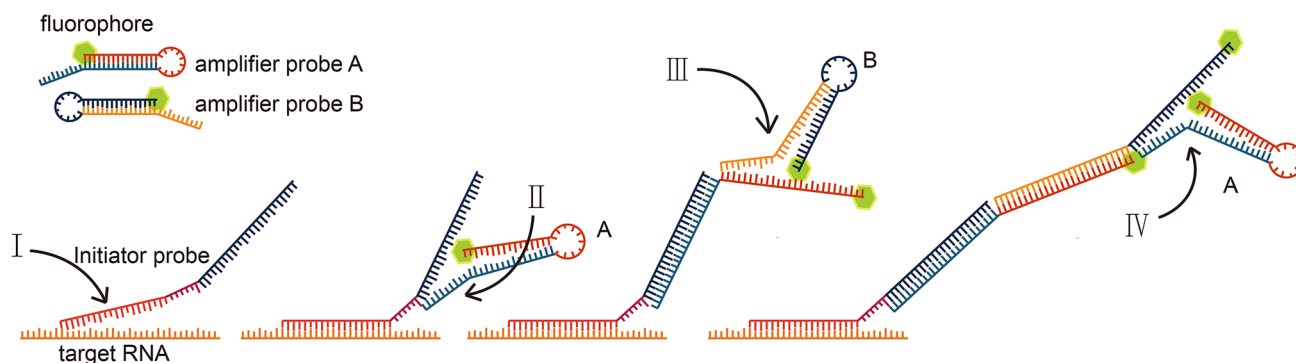

Fig. 1 Mechanism of HCR-FISH. After the initiator probe hybridized to the target RNA (process I), amplifier probes could bind to the initiator step by step (process II, III, IV) (Dirks and Pierce 2004; Yamaguchi et al. 2015b)

of probe B, releasing a sequence identical to the initiator sequence that can also bind to probe A (Fig. 1, process III). Thus, the fluorescence-labeled amplifier probes A and B accumulate around the target sites in a form of elongated double-stranded DNA with a strong fluorescence signal (Fig. 1, process IV). Yamaguchi et al. (2015b) first applied HCR-FISH on environmental microbes, validating it by using it on active sludge samples. Nikolakakis et al. (2015) used HCR-FISH to observe the migration of syntrophic microbes on squids. Recently, Imachi et al. (2020) successfully enriched strains of Asgard archaea and documented their shapes using HCR-FISH. There are several advantages of using HCR-FISH compared to CARD-FISH. Firstly, the probes in HCR-FISH are much smaller, and so can more easily penetrate the cells (Amann and Fuchs 2008). Secondly, the fluorophores are labeled on amplifier probes rather than initiator probes, thus the initiator probes can easily be changed with demand with only a small additional cost of time and expense. Thirdly, not using H_2O_2 in the HCR-FISH protocol better preserves the target RNA in the sample (Massie et al. 1972). Fourthly, the HCR-FISH protocol is less time-consuming.

While the signal intensity of FISH can be improved by the above methods, the specificity of FISH can be influenced by additional factors, especially in sediment samples. Firstly, if the hybridization condition is not stringent enough, the probe may bind to non-targeted RNAs with partially complementary sequences. If this occurs, cells without target RNA may also present a probe signal. Secondly, although base-pair matching does not occur, there is still a chance that the probe will be adsorbed by abiotic particles (Amalfitano and Fazi 2008; Daims and Wagner 2007). This would be more likely in HCR-FISH as more DNA probes are involved, increasing the possibility of DNA adsorption by abiotic particles. These kinds of problems prevent the application of HCR-FISH to sediment and soil samples. Indeed, one attempt to apply HCR-FISH to sediments was unsuccessful due to strong false-positive signals (Buongiorno et al. 2017). In this study, we first validated and optimized HCR-FISH on pure cultures of the bacterium *Escherichia coli* and the archaeon *Methanococcoides methylutens*. We found that the concentration of the initiator probe in the hybridization buffer needed to be increased to 10 µmol/L and two sets of HCR sequences outcompeted others. Then, we tried to reduce the false positive rate of HCR-FISH on sediment samples. Modifications regarding pretreatment methods and hybridization reagents were validated for sediment samples. We also developed an image-processing method that could improve the performance of DAPI counter staining. Combining these methods, we successfully visualized microbes in sediment with HCR-FISH, demonstrating HCR-FISH as a promising method for use in environmental microbial community research.

Results and discussion

Verification of HCR-FISH on pure-cultured microbes

Modification of the HCR-FISH protocol

To verify the protocol, HCR-FISH was first tested on the model bacterium *E. coli,* targeted by the universal bacterial probe EUB338, following the procedure proposed by Yamaguchi et al. (2015a, b). In the original protocol, the concentration of initiator probe was 1 µmol/L, similar to that used in the traditional FISH. In these conditions, the signal of HCR-FISH on *E. coli* was too unclear to identify the exact location and shape of individual cells (Fig. 2a–c). The cell signal became more intensive and clearer when the probe concentration was increased from the original 1 µmol/L to 2.5 or 10 µmol/L (Fig. 2d–i). Other modifications of the fixation procedure and hybridization state, including the temperature, formamide concentration and moisture level, etc., did not show much improvement when the concentration of the initiator probe remained at 1 µmol/L (data not shown). Therefore, the concentration of initiator probe in the hybridization buffer was set to 10 µmol/L for all further experiments. The average fluorescence signal intensity of HCR-FISH on *E. coli* (8.85 ± 1.3 arbitrary unit, A.U.) was ~ 5 times that of traditional FISH (1.61 ± 0.58 A.U.) and there were no obvious differences between the cell counting results on *E. coli* by HCR-FISH (($6.74 \pm 2.14) \times 10^8$ cells/ml) and by SYBR Green I staining (($7.56 \pm 3.25) \times 10^8$ cells/ml) (Student's *t*-test, $n1 = n2 = 3$, $P > 0.1$). The modified protocol also worked well on pure cultures of the archaeon *Methanococcoides methylutens* (Fig. 2j–l). While several groups have independently conducted the HCR-FISH protocols of Yamaguchi et al. (2015a, b), they did not arrive at a unified conclusion on the suitability of this protocol (Buongiorno et al. 2017; Francis et al. 2019; Grieb et al. 2020; Matsubayashi et al. 2017; Royet et al. 2018). Therefore, it is likely that some experimental conditions suggested in the Yamaguchi et al. (2015a, b) protocols are only marginally suitable and may need further optimization to achieve robust performance. Here, it is proposed that increasing the concentration of the initiator probe in the hybridization buffer improves the original protocol. In this study, the method was validated by two relatively independent labs.

Test of HCR probe sets

Observing phylogenetically distinct microbes simultaneously allows more application of HCR-FISH. In order to achieve this goal, at least two sets of HCR sequences are
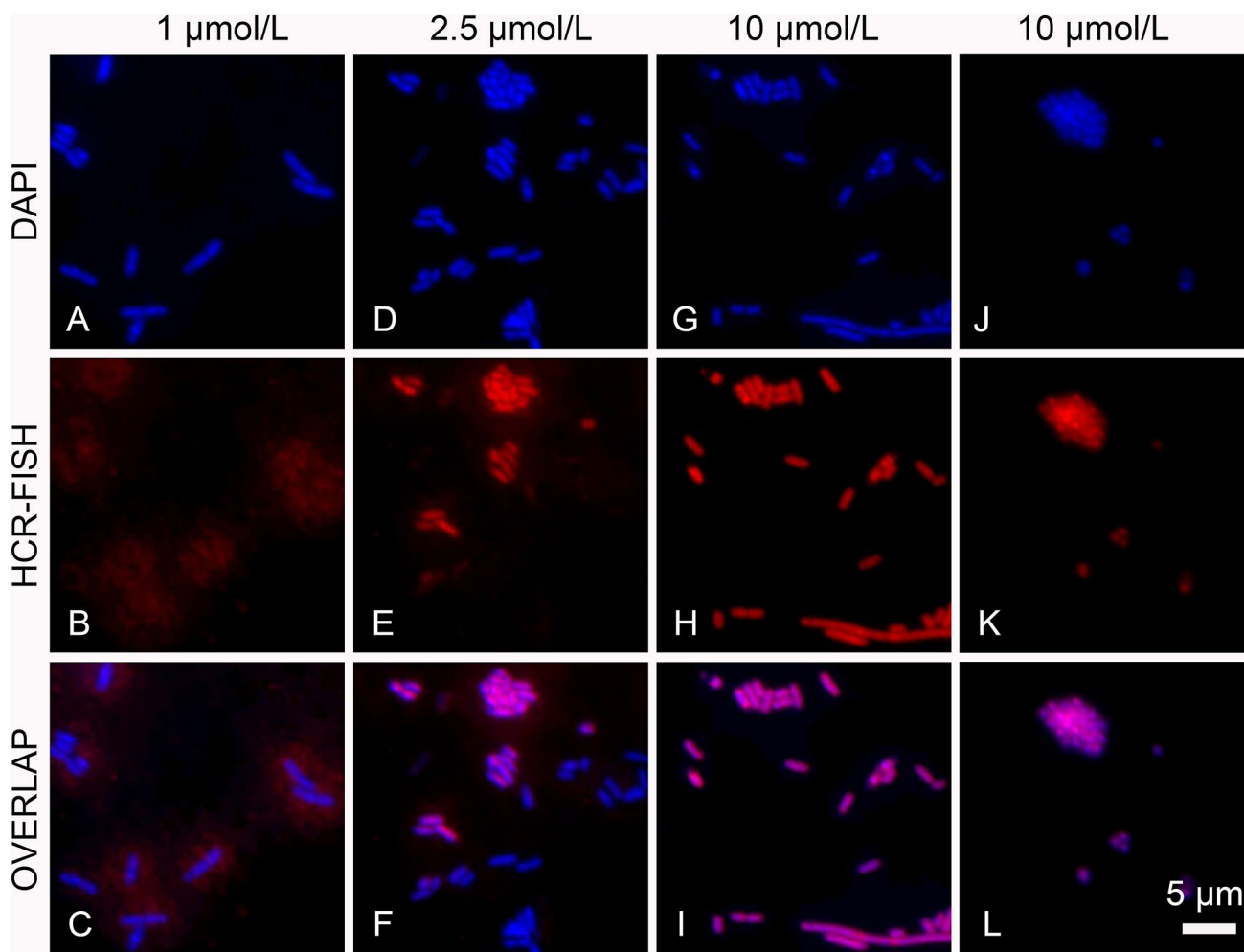
Fig. 2 HCR-FISH on pure cultured microbes. *E. coli* was labeled with EUB338 (**a–i**) and *M. methylutens* was labeled with ARCH915 (**j–l**), both with HCR probe set S1. The concentrations of initiator probe in hybridization solution are 1 µmol/L (panel **a–c**), 2.5 µmol/L (panel **d–f**), and 10 µmol/L (panel **g–l**), respectively. The micrographs depict DAPI stain (left) and those depict HCR-FISH signals (middle) are overlapped on the right

required and they should meet the following criteria: (a) these sequences should be orthogonal, meaning that they won't hybridize with each other; and (b) using identical protocols, they should give an acceptable performance under the same working conditions, i.e., they will give a strong signal with the targeted microbes and weak signals with the untargeted materials. Based on previous studies (Choi et al. 2014; Yamaguchi et al. 2015b), five orthogonal HCR sequence sets named S1/S2/S3/L1/L2 (Table 1) were chosen and tested on *E. coli*. Those that worked well under the modified protocol were selected for further experiments. Among them, S1, S2, and S3 were shorter in length, with initiator sequences consisting of 26 nucleotides, while those of L1 and L2 had 36 nucleotides each. Each initiator sequence was fused with bacterial universal probe EUB338. It was revealed that the shorter probe sets, S1 and S2, gave stronger fluorescence signals, while L1 and L2 emitted only vague

and unclear signals, similar to the results of the S1 probe using a probe concentration of 1 µmol/L (Supplementary Fig. S1a, b). It is possible that the shorter length gave S1 and S2 a better opportunity to enter the cells and interact with their targeted RNA, while a longer length made L1 and L2 more likely to be influenced by steric factors. Based on these results, experiments with L1 and L2 were discontinued. The S3 probe set resulted in many nonspecific binding signals outside the cells (Supplementary Fig. S1c), consistent with a previous study (Buongiorno et al. 2017). Comparatively, the presence of S1 and S2 signals were well limited in the neighborhood of DAPI signal, showing high specificity (Fig. 2g–i, Supplementary Fig. S1d). It's possible that the sequence of S3 itself tended to trigger nonspecific binding. At last, probe S1 and S2 were selected for further study because of their high signal intensity, clearness, and specificity.

Table 1 Probes used in this study

Probe name	Probe sequence (5′-3′)	Reference
S1a	TCTAGTCGTTGATGCTTTGTATTCGGCGACAGATAACCGAATACAAAGCATC	Choi et al. (2010)
S1b	CCGAATACAAAGCATCAACGACTAGAGATGCTTTGTATTCGGTTATCTGTCG	Choi et al. (2010)
S2a	CATAGGGTTCGGATTCTTAGGGCGTAGCAGCATCAATACGCCCTAAGAATCC	Choi et al. (2010)
S2b	TACGCCCTAAGAATCCGAACCCTATGGGATTCTTAGGGCGTATTGATGCTGC	Choi et al. (2010)
S3a	ATGAAGGACGGACTACTGATAACTGGGACTTCCATACCAGTTATCAGTAGTC	Choi et al. (2010)
S3b	CCAGTTATCAGTAGTCCGTCCTTCATGACTACTGATAACTGGTATGGAAGTC	Choi et al. (2010)
L1a	GAAGCGAATATGGTGAGAGTTGGAGGTAGGTTGAGGCACATTTACAGACCTCAACCT ACCTCCAACTCTCAC	Choi et al. (2014)
L1b	CCTCAACCTACCTCCAACTCTCACCATATTCGCTTCGTGAGAGTTGGAGGTAGGTTG AGGTCTGTAAATGTG	Choi et al. (2014)
L2a	CGGGTTAAAGTTGAGTGGAGATATAGAGGCAGGGACAAAGTCTAATCCGTCCCTGCC TCTATATCTCCACTC	Choi et al. (2014)
L2b	GTCCCTGCCTCTATATCTCCACTCAACTTTAACCCGGAGTGGAGATATAGAGGCAGG GACGGATTAGACTTT	Choi et al. (2014)
ARCH915-S1	CCGAATACAAAGCATCAACGACTAGAAAAAAGTGCTCCCCGCCAATTCCT	Yamaguchi et al. (2015a, b)
ARCH915-S3	CCAGTTATCAGTAGTCCGTCCTTCATTTTTTGTGCTCCCCGCCAATTCCT	This study
EUB338-S1	CCGAATACAAAGCATCAACGACTAGAAAAAAGCTGCCTCCCGTAGGAGT	Yamaguchi et al. (2015a, b)
EUB338-S2	TACGCCCTAAGAATCCGAACCCTATGAAAAAGCTGCCTCCCGTAGGAGT	This study
EUB338-S3	CCAGTTATCAGTAGTCCGTCCTTCATTTTTTGCTGCCTCCCGTAGGAGT	This study
EUB338-L1	GTCCCTGCCTCTATATCTCCACTCAACTTTAACCCGAAAAAAGCTGCCTCCCGTAGG AGT	This study
EUB338-L2	CCTCAACCTACCTCCAACTCTCACCATATTCGCTTCAAAAAAGCTGCCTCCCGTAGG AGT	This study
ANME-1-350-S1	CCGAATACAAAGCATCAACGACTAGAAAAAAAGTTTTTCGCGCCTGATGC	This study
SEEP2-658-S2	TACGCCCTAAGAATCCGAACCCTATGAAAAATCCACTTCCCTCTCCGGT	This study

Decreasing the negative effects of abiotic particles on HCR-FISH

Through sorption of probes and fluorophores, abiotic particles in sediment significantly interfere with the performance of traditional FISH and HCR-FISH. Furthermore, large quantities of abiotic particles can cover the microbes during cell embedding (on a filter membrane), causing problems for observation. These negative effects can be alleviated by reducing either the number of abiotic particles or the adsorption of abiotic particles on the probes. To reduce these negative effects several methods for improving the performance of FISH on sediments were tested.

Removal of abiotic particles

Sediment particles and cells can be easily separated due to their large differences in density, but first, the cells need be detached from the abiotic particles by physical and/or chemical means to avoid cell loss during separation. Several detachment methods were tested on paraformaldehyde-treated sediment samples. Method A uses a buffer with detergent to wash the cells off the abiotic particles, while method B uses an ultrasonic probe (Kallmeyer et al. 2008). Both methods were evaluated by counting the total cell number in their supernatant after an hour of precipitation. The cell counting results obtained using methods A, B and that result of the control group were 5.70 ± 1.89, 3.20 ± 0.52, 2.80 ± 0.25 per nanoliter, respectively. Compared with the untreated sample, more cells were obtained in the supernatant through method A (Student's t-test, $n1 = n2 = 5$, $P < 0.01$), whereas method B had no obvious effect (Student's t-test, $n1 = n2 = 5$, $P > 0.1$).

For the separation step, a multi-layer density gradient centrifugation method was tested on samples treated with method A. Multiple density layers were thought to help avoid the co-precipitation of microbes with abiotic particles in the turbulent flow caused by falling of abiotic particles (Morono et al. 2013). Compared with the group that only stood still for one hour as separation, density gradient centrifugation yielded higher cell numbers, and less cells remained in the pellet (Table 2). Thus, multi-layer density gradient centrifugation was adopted in the protocol for cell separation in further experiments.

Table 2 Performance of different extraction methods on sediment samples from South China Sea

Cell number (10^5cells/ml)	DG	Control
Supernatant	18.55 ± 2.94	4.30 ± 1.54
Pellet	4.51 ± 1.07	8.74 ± 1.07

DG density gradient centrifugation method. The number of cells in the supernatant and pallet after centrifugation was counted separately. See Supplementary Table S1 for more information

Reducing the sorption of initiator probe by abiotic particles

To reduce false-positive signals resulting from the nonspecific binding of abiotic particles on probes, three types of hybridization buffer (A, B, C) were tested (Table 3). Buffer A is a widely used formula for FISH on environmental samples (Yamaguchi et al. 2015b). Buffer B is mostly used with eukaryote samples, with several traditional blocking reagents amended (Choi et al. 2014). Buffer C contains a high concentration of EDTA (Morono et al. 2020). Our experiments demonstrated that Buffer B did not work well on sediment samples, as nonspecific binding remained significant. The performance of Buffer C outcompeted that of Buffer A in decreasing the nonspecific binding. Buffer C was thus selected for further experiments.

Imaging and image processing to reduce false counterstaining signal

In FISH experiments, DNA counterstaining is often applied to locate cells. A widely used counterstaining dye is DAPI, which shows specificity on double-stranded DNA. However, sediment particles, with complex compositions and structures, inevitably absorb DAPI molecules and emit a background fluorescence signal. In practice, using one band-pass DAPI filter set, it is difficult to differentiate cells and abiotic particles based solely on their shape and intensity. Similarly, the DNA dye SYBR Green is also absorbed by abiotic particles, although it was found that the emission spectrum of SYBR Green goes through a redshift when it binds to abiotic particles rather than DNA (Sunamura et al. 2003). By using a band-pass filter 490/20 nm (center wavelength/bandwidth) for excitation and 528/38 nm and 617/73 nm filters for detection, abiotic particles could easily to be ruled out (Morono et al. 2009). However, SYBR Green produces signals under several fluorescence channels and thus may not be compatible with FISH.

In the hope that DAPI might have similar properties to SYBR Green, several filter sets were tested. Our results showed that DAPI-DNA complex only emitted a bright signal under light filter UV-2A (excitation filter 355/50 nm, dichroic mirror 400 nm, barrier filter 410 nm), while the DAPI-abiotic-particle complex emitted signals both under UV-2A and BV-2A (excitation filter 420/40 nm, dichroic mirror 455 nm, barrier filter 460 nm). Based on this property, images under UV-2A (Fig. 3a) and BV-2A (Fig. 3b) were acquired, separately, then the latter images were subtracted from the former. This process was able to dramatically decrease the signal of abiotic particles, while still retaining the signal of cells (Fig. 3c). The spectrum shift of the DAPI signal on abiotic particles may be related to the fact that DAPI has two binding modes to DNA, each of which has an independent fluorescence spectrum and fluorescence quantum yield (Manzini et al. 1983). According to previous studies, mineral particles in the sediment sample can absorb debris DNA to become DAPI-bindable (Krsek and Wellington 1999). It is possible that DAPI bindings to debris DNA and genomic DNA have different preferences for binding modes. The different ratio of each type of binding modes on debris DNA and genomic DNA may cause the shift of spectrum.

Table 3 Composition of hybridization buffer tested on sediment samples

| Main ingredients	Hybridization buffer A	Hybridization buffer B	Hybridization buffer C
Tris–HCl	20 mmol/L	–	20 mmol/L
EDTA	0	–	250 mmol/L
SDS	0.01% (w/v)	–	0.01% (w/v)
NaCl	0.9 mol/L	–	–
Dextran sulfate	10% (w/v)	10% (w/v)	–
5× Sodium chloride sodium citrate	–	5×	–
Citric acid	–	9 mmol/L	–
1× Denhardt' solution	–	1×	–
Tween 20	–	0.1% (v/v)	–
Heparin	-	50 µg/ml	–
Formamide	X% (v/v)	X% (v/v)	X% (v/v)
reference	Yamaguchi et al. (2015a)	Choi et al. (2014)	Morono et al. (2020)
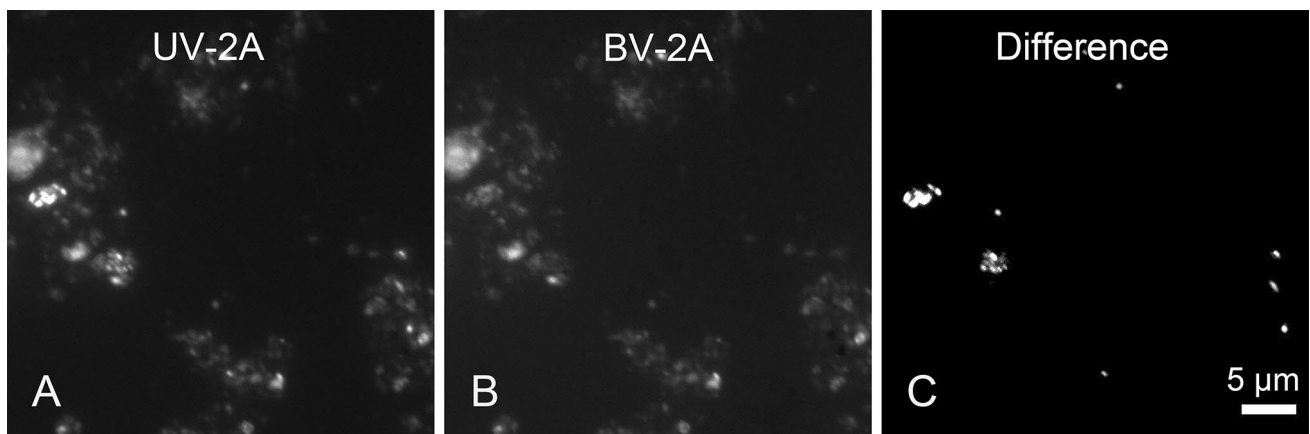
Fig. 3 Image processing excludes false positive signal of DAPI stain. Image taken from UV-2A channel (**a**) subtracts that taken from BV-2A channel (**b**) to produce a new image with enhanced signal of cells and decaying signal of abiotic particles (**c**)

Detecting microbial cells in sediment samples

After improving the performance of HCR-FISH on sediment samples, an optimized protocol was proposed (Supplementary Table S1 and Fig. 5). A sediment sample from the South China Sea and an anaerobic methanotroph enrichment from the Guaymas Basin sediment (Krukenberg et al. 2018) were further tested using the optimized protocol as shown in Fig. 5. After HCR-FISH, samples were counterstained with DAPI and microscopically examined. A post-imaging process was necessary to discriminate cells from fluorescent abiotic particles. As shown in Fig. 4, microbial cells could be clearly visualized by HCR-FISH, both on sediments from South China Sea and the enrichment slurry sample. For the South China Sea sample, traditional FISH was also applied for comparison. The average fluorescence intensity of the signals from bacteria were 10.9 ± 2.1 and 1.79 ± 0.60 A.U. through HCR-FISH and traditional FISH, respectively. There is thus a $\sim 6\times$ elevation of signal intensity using the HCR process. It was also noteworthy that, although multi-layer density gradient centrifugation was applied to this sample, many abiotic particles still remained. This indicates that many abiotic particles have a similar density to the cells. During cell embedding (on a filter membrane), the accumulation of these types
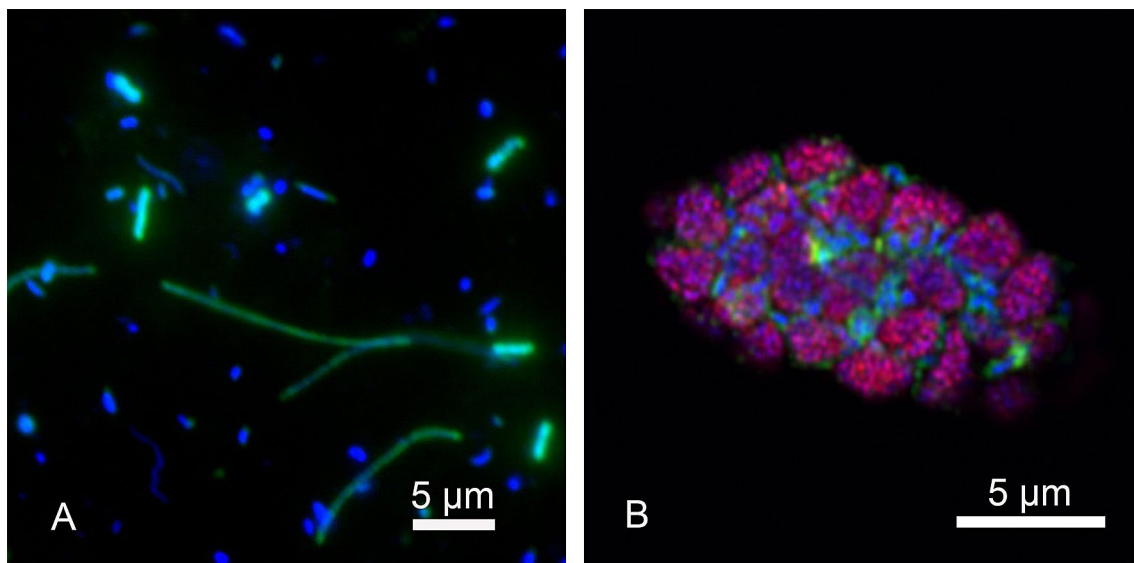

Fig. 4 HCR-FISH on two environmental samples. **a** HCR-FISH on sediment sample from South China Sea. Bacteria were labeled by EUB338-S1. Scale bar, 5 μm. **b** HCR-FISH on an enrichment sample of anaerobic methanotrophic archaea (ANME) consortia. SRB and ANME were labeled by species-specific probe SEEP2-658-S1 and ANME-1-350-S2, respectively
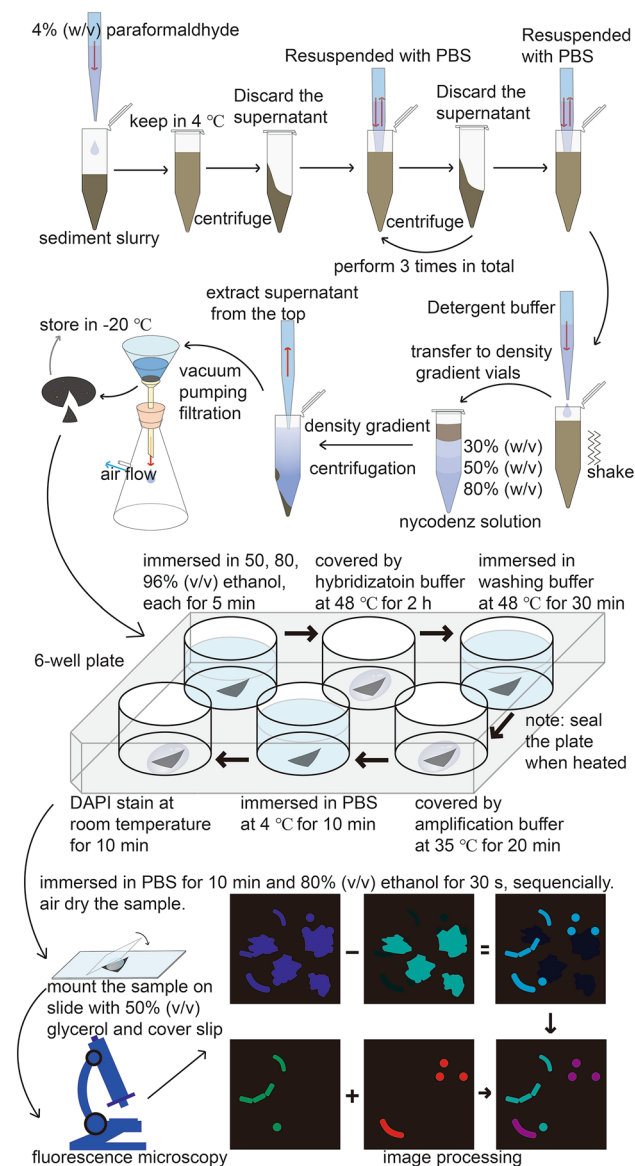
Fig. 5 Cartoon showing the complete protocol of HCR-FISH on sediment sample. The sediment slurry is fixed by paraformaldehyde and then washed with PBS. Cells are detached through shaking in the detergent buffer and extracted through density gradient centrifugation. 0.22 μm-pore-size polycarbonate membrane is used for capturing cells. A piece of membrane is placed in the container like a 6-well plate. After dehydration with series ethanol solution, the air-dry membrane is covered by hybridization buffer and amplification buffer sequentially, each followed a washing step. Then the sample is stained with DAPI and mounted on the slide for microscopy. The image taken under BV-2A channel was subtracted from that under UV-2A channel for cell recognition and counting. The result could be overlaid with FISH probe signals for further analysis

of abiotic particles will also cover the cell, making the improvement by density gradient centrifugation less than expected.

Potential of HCR-FISH

In addition to the application to marine sediment samples, our modified protocol may also be directly applied to concentrated seawater samples, which share the same features of low cellular rRNA content. The 6× signal enhancement ensures a better sensitivity of HCR-FISH than that of traditional FISH. The better penetration performance makes HCR-FISH more competitive on unknown samples than CARD-FISH, whose permeabilization process is empirical and sample dependent (Amann and Fuchs 2008). Meanwhile, the DAPI-related image processing method could also be integrated into other fluorescence imaging experiments, including CARD-FISH and auto-fluorescence observation, to help identify cells from false-positive signals.

In addition to detecting microbes, single-cell level detection of mRNA can be more appealing to researchers studying unculturable microbes. For example, study of *mcr*A transcripts in methanogens using a two-step CARD-FISH process (i.e., two-pass Tyramide Signal Amplification FISH) shows the possibility to detect mRNA in microbes by FISH (Kubota et al. 2006). However, this method has not been widely used, probably because of its complexity. Some studies have used single-molecular FISH (smFISH), a method that involves a set of more than 40 probes targeting different regions on the sequence of mRNA (Sepulveda et al. 2016; Skinner et al. 2013; So et al. 2011; Taniguchi et al. 2010; Yang et al. 2019), to locate mRNA molecules inside *E. coli*. Furthermore, genes could also be visualized by signal-enhanced FISH like virusFISH (Castillo et al. 2020) or geneFISH (Barrero-Canosa et al. 2017; Moraru et al. 2010), which combines the strategies of dense fluorescent labeling of single probe and multiple probes. Considering the success of CARD-FISH and smFISH on in situ detection of single molecules in microbes, it would also be expected that HCR-FISH would be an effective single-molecule detection tool based on its efficient signal amplification and relatively easy protocol.

Conclusions

The traditional FISH, with a single probe, was not sensitive enough to explore tiny and/or less active microbes in many natural environments, such as marine sediments (Ishii et al. 2004) and open ocean seawater (Morris et al. 2002). Several new technologies have been developed to deal with this problem. In this study, we have demonstrated that HCR-FISH, one of these technologies, can significantly improve the labeling of microbes in sediment samples. The overall performance of the original HCR-FISH on sediment samples could be improved by applying the following modifications: 1) The signal intensity and resolution of HCR-FISH can be

optimized through changing the concentration of initiator probes and types of HCR sequences; 2) The negative effects of abiotic particles in HCR-FISH of sediment samples can be reduced by employing sample pretreatment and optimized hybridization buffer; 3) The counterstaining signal of cells could be distinguished from the background fluorescence of abiotic particles by performing an image processing method to emphasize the cellular DAPI signal. Combining these efforts, we developed an optimized HCR-FISH protocol for sediment samples (Supplementary Table S1 and Fig. 5).

Materials and methods

Sample preparation

E. coli and *M. methylutens* were selected as representatives of bacteria and archaea, respectively. *E. coli* DH5α was cultured in Luria–Bertani (LB) broth at 37 ℃ under 200 rpm shaking. *M. methylutens* DSM 16625 was obtained from the German Collection of Microorganisms and Cell Cultures (DSMZ, Braunschweig, Germany) and cultured according to DSMZ protocols. Cells were fixed in 4% (v/v) paraformaldehyde with phosphate-buffered saline (PBS; 136 mmol/L NaCl, 2.6 mmol/L KCl, 8 mmol/L Na_2HPO_4, and 2 mmol/L KH_2PO_4 [pH 7.2]) for 6 h at 4 ℃, washed twice by PBS, and preserved in PBS/ethanol 1:1 (v/v) mixture at −20 °C.

Sediment samples were collected from the South China Sea and stored at −80 °C before proceeding to HCR-FISH. The same fixation and preservation procedures, as described above and in Supplementary Table S1, were applied on these sediment samples.

An enrichment sample of anaerobic methanotroph was transferred from a long-term enrichment incubator at the Max Planck Institute for Marine Microbiology, Germany. The enrichment was transferred and refreshed according to the reference (Krukenberg et al. 2018). The same fixation and preservation procedures, as described above and in Supplementary Table S1, were also applied.

Cell detachment

Cells were detached from fixed samples using different methods. For method A, eight volumes of sediment were mixed with one volume of detergent buffer (100 mmol/L EDTA, 100 mmol/L sodium pyrophosphate, 1% (v/v) Tween 80) and vortexed for one hour at level 5 (Vortex-Genie 2, Scientific Industries). For method B, samples were placed in an ice-water mixture 2 cm away from an ultrasonic probe (Model 50 Sonic Dismembrator, Thermofisher). A 30-s sonication with 50% maximum power was performed three times, each followed by a resting period of 30 s. To evaluate their performance, detached samples were rested for an

hour to precipitate the particles, and the supernatant was used for the cell counts. A control group was also set with fixed sediment sample shaken, rested, and counted as for the other groups.

Cell extraction

Cells were extracted from the detergent buffer detached samples with density gradient centrifugation. Samples were centrifuged at 1500 *g* for 30 min through multiple density layers consisting of 30%, 50%, and 80% (w/v) Nycodenz (Axis-Shield, Norway), respectively. All the transparent liquid was carefully transferred to a clean vial to avoid the disturbance on the precipitate. Then, the supernatant was diluted 4 times by PBS and centrifuged at 14,500 *g* for 15 min to collect the cells. The precipitated cells were resuspended in PBS for further processing. To compare, parts of the detached samples were allowed to stand for an hour to precipitate the abiotic particles and suspend cells. Their supernatants were collected and stored in PBS for further processing.

Cell counting

To capture the cells, pretreated samples were first diluted in 10 ml PBS and then filtered onto 0.22 μm pore size membranes (GTBP02500, Isopore, Merck Millipore). Then, the membrane was dipped in 50, 80, and 96% (v/v) ethanol for dehydration, each step was for 5 min (Yamaguchi et al. 2015a). SYBR Green I (Solarbio, China) was diluted in ultrapure water by 100 times to provide the working solution. The working solution was then applied to the membranes containing the samples for 10 min at room temperature. Then, the membranes were placed on the top of the delicate task wipes (Kimtech Science, USA). The remaining working solution would be absorbed by the delicate task wipes. For each filter membrane, 16 fields of view were selected and counted under the microscope. Three filter membranes were analyzed per sample.

HCR-FISH

The HCR-FISH protocol was modified based on that of Yamaguchi et al. (2015a). Cells were captured on membranes as described in "Cell counting" section. The membrane was cut into eight pieces, each of which was enough for the following experiment. The unused pieces were stored in −20 °C for future usage. 40 μl of hybridization buffer with 10 μmol/L initiator probes was added to the membrane. The concentration of formamide in the hybridization buffer depends on the sequence of the probe. As tested here, 25% (v/v) formamide was acceptable for simultaneous detection of microbes using probe EUB338, ARCH915, ANME-1-350 and SEEP2-658. The sample was incubated at 46 °C for 2 h

Table 4 Filter information of light filter cubes in microscope for this study

	Excitation filter	Dichroic filter	Barrier filter
UV-2A long-pass filter set	355/50 nm[a]	400 nm	410 nm
BV-2A long-pass filter set	420/40 nm	455 nm	460 nm
DAPI band-pass filter set	375/28 nm	415 nm	460/60 nm
FITC band-pass filter set[b]	480/30 nm	505 nm	535/45 nm
Texas Red band-pass filter set[c]	560/40 nm	595 nm	630/60 nm

[a]Central wavelength/bandwidth, the same hereinafter

[b]Used for fluorophore Alexa 488

[c]Used for fluorophore Alexa 594

in humidified conditions. The humidity requirement can be achieved by sealing the sample in a small container and/or placing a wet tissue beside the sample. After incubation, the membrane was washed in 10 ml washing buffer [20 mmol/L Tris–HCl, 0.01% (w/v) SDS, 0.056–0.225 mol/L NaCl] and incubated at 48 ℃ for 30 min to remove excessive initiator probes. The concentration of NaCl in the washing buffer depends on the concentration of formamide in the hybridization buffer. Based on the Pernthaler et al. (2001), 0.056 mol/L NaCl was used for 40% (v/v) formamide, 0.159 mol/L NaCl for 25% (v/v) formamide and 0.225 mol/L NaCl for 20% (v/v) formamide. A complete table of concentration pairs can be found in Pernthaler et al. (2001). All the following steps should be done in dark to avoid quenching of the fluorophore. During washing, each amplifier probe was dissolved in amplification buffer [0.9 mol/L NaCl, 0.05 mol/L Na_2HPO_4, 0.01% (w/v) SDS] and incubated stepwise at 95 °C for 90 s and 25 °C for 30 min, for initialization. Next, these amplifier probes were mixed and the final concentration of each probe was 2.5 µmol/L. 30 min later, the washing buffer was removed and 40 µl amplifier probes mixed with amplification buffer was added to the membrane. The membrane was then incubated at 35 °C for 20 min under humidified conditions. Sequentially, 10 ml 4 °C PBS was applied to the membrane on ice to remove excessive fluorescent probes. The membrane was washed in ultrapure water and then in 96% (v/v) ethanol each for one minute on ice and air-dried.

For counterstaining, 20 µl of 10 ng/ml DAPI was applied to the samples for at least 10 min. Samples were washed by PBS for 10 min and dehydrated by 80% (v/v) ethanol.

Traditional FISH

Samples underwent the same treatment as those in the HCR-FISH protocol until the hybridization step. 40 µl of hybridization buffer with 10 µmol/L of fluorophore-labeled probes was added to the membrane. The sample was incubated and washed following the same procedure as for HCR-FISH. Then, the membrane was directly washed in water and 96%

(v/v) ethanol, each for one minute, on ice and air dried. The counterstaining step remained the same.

Imaging and image processing

The imaging experiment was carried out by epifluorescence microscope (Nikon ECLIPSE 90i, Tokyo, Japan), coupled with an illuminator (Nikon INTENSILIGHT C-HGFIE, Tokyo, Japan) and a CCD camera (CoolSNAP HQ2, Photometrics, USA). Nikon plan-apochromat 100× oil objective lens was used for imaging. The excitation filter, dichroic filter, and barrier filter of light filter cubes are summarized in Table 4. The camera exposure time varied between 50 and 800 ms depending on the type of fluorophore and observed samples. Images of anaerobic methanotrophs were collected with a Zeiss LSM 880 microscope (Carl Zeiss, Germany) equipped with a plan-apochromat 63× oil objective lens and Airyscan super-resolution system for better resolution. 405, 561, and 633 nm lasers were used for excitation of DAPI, Alexa Fluor 555, Alexa Fluor 647, respectively.

The channel subtraction was performed using the Image Calculator function integrated in Fiji (a "batteries-included" distribution of ImageJ 1.53c) software released on 2017 May 30 (Schindelin et al. 2015). To balance the background differences between channels, the images were treated under the following rules: define the gray value that most pixels possessed for images from UV-2A and BV-2A channels as I_U and I_B, respectively. Both I_U and I_B represent the low-intensity background in the corresponding image channels. Hence, pixels with a grey level of I_U in UV-2A channel and those with grey level of I_B in BV-2A channel should occupy the same positions in the image. Then, the grey values of these pixels should become zero by channel subtraction to precisely eliminate the background signal. This could be achieved by multiplying the grey value of each pixel on the image from BV-2A by a factor $\alpha = I_U/I_B$. Practically, $\alpha \approx 1/8$ for our instruments, and thus the goal could also be achieved by adjusting the exposure time or exciting light intensity for an image from BV-2A to 1/8 of that of the image from UV-2A. The factor α may vary with different light sources, but not with samples.

The analysis of cellular fluorescence intensity was also performed on Fiji. To identify the region of positive signal for each channel, two binary images were created from the channel-subtracted DAPI image and (HCR-)FISH image, separately. The thresholds for producing these binary images were decided based on the built-in automatic algorithm "Moments". The intersection of the two binary images was used as the cellular mask for intensity calculation of true cells. To measure the cellular fluorescence intensity, we first designated the (HCR-)FISH image to be calculated in the "Set Measurements…" window. Then the window of the cellular mask image was activated and the "Analyze Particles" function was run. The "target size" parameter of the function was set to be 0.5–100 mm^2. With this pipeline, the Fiji software would first mark the cell regions using the cellular mask image, and then calculate the average grey value of each region on the (HCR-)FISH image. For each experiment group, at least 200 cells were taken into account.

Declarations

References

Amalfitano S, Fazi S (2008) Recovery and quantification of bacterial cells associated with streambed sediments. J Microbiol Methods 75:237–243

Amann R, Fuchs BM (2008) Single-cell identification in microbial communities by improved fluorescence *in situ* hybridization techniques. Nat Rev Microbiol 6:339–348

Amann RI, Ludwig W, Schleifer K-H (1995) Phylogenetic identification and in situ detection of individual microbial cells without cultivation. Microbiol Rev 59:143–169

Bao J, Zhang W, Zhou W, Lv M, Lu C, Yu H (2020) An amplification strategy for detecting HER2 with a quasi-targeted proteomics approach coupled with aptamer-triggered hybridization chain reaction. Talanta 215:120918

Baptista JD, Lunn M, Davenport RJ, Swan DL, Read LF, Brown MR, Morais C, Curtis TP (2014) Agreement between *amoA* gene-specific quantitative PCR and fluorescence *in situ* hybridization in the measurement of ammonia-oxidizing bacteria in activated sludge. Appl Environ Microbiol 80:5901–5910

Barrero-Canosa J, Moraru C, Zeugner L, Fuchs BM, Amann R (2017) Direct-geneFISH: a simplified protocol for the simultaneous detection and quantification of genes and rRNA in microorganisms. Environ Microbiol 19:70–82

Bi S, Yue SZ, Zhang SS (2017) Hybridization chain reaction: a versatile molecular tool for biosensing, bioimaging, and biomedicine. Chem Soc Rev 46:4281–4298

Buongiorno J, Turner S, Webster G, Asai M, Shumaker AK, Roy T, Weightman A, Schippers A, Lloyd KG (2017) Interlaboratory quantification of Bacteria and Archaea in deeply buried sediments of the Baltic Sea (IODP Expedition 347). FEMS Microbiol Ecol 93:fix007

Castillo YM, Sebastian M, Forn I, Grimsley N, Yau S, Moraru C, Vaque D (2020) Visualization of viral infection dynamics in a unicellular eukaryote and quantification of viral production using virus fluorescence *in situ* hybridization. Front Microbiol 11:1559

Chen Y, Li YL, Zhou GT, Li H, Lin YT, Xiao X, Wang FP (2014) Biomineralization mediated by anaerobic methane-consuming cell consortia. Sci Rep 4:5696

Choi HM, Chang JY, le Trinh A, Padilla JE, Fraser SE, Pierce NA (2010) Programmable *in situ* amplification for multiplexed imaging of mRNA expression. Nat Biotechnol 28:1208–1212

Choi J, Love KR, Gong Y, Gierahn TM, Love JC (2011) Immuno-hybridization chain reaction for enhancing detection of individual cytokine-secreting human peripheral mononuclear cells. Anal Chem 83:6890–6895

Choi HMT, Beck VA, Pierce NA (2014) Next-generation *in situ* hybridization chain reaction: higher gain, lower cost, greater durability. ACS Nano 8:4284–4294

Daims H, Wagner M (2007) Quantification of uncultured microorganisms by fluorescence microscopy and digital image analysis. Appl Microbiol Biotechnol 75:237–248

Dirks RM, Pierce NA (2004) Triggered amplification by hybridization chain reaction. Proc Natl Acad Sci USA 101:15275–15278

Fazi S, Amalfitano S, Pizzetti H, Pernthaler J (2007) Efficiency of fluorescence in situ hybridization for bacterial cell identification in temporary river sediments with contrasting water content. Syst Appl Microbiol 30:463–470

Francis TB, Krüger K, Fuchs BM, Teeling H, Amann RI (2019) Candidatus *Prosiliicoccus vernus*, a spring phytoplankton bloom associated member of the Flavobacteriaceae. Syst Appl Microbiol 42:41–53

Gao Z, Qiu Z, Lu M, Shu J, Tang D (2017) Hybridization chain reaction-based colorimetric aptasensor of adenosine 5'-triphosphate

on unmodified gold nanoparticles and two label-free hairpin probes. Biosens Bioelectron 89:1006–1012

Grieb A, Bowers RM, Oggerin M, Goudeau D, Lee J, Malmstrom RR, Woyke T, Fuchs BM (2020) A pipeline for targeted metagenomics of environmental bacteria. Microbiome 8:21

Hatzenpichler R, Connon SA, Goudeau D, Malmstrom RR, Woyke T, Orphan VJ (2016) Visualizing in situ translational activity for identifying and sorting slow-growing archaeal-bacterial consortia. Proc Natl Acad Sci USA 113:E4069-4078

Hou T, Li W, Liu X, Li F (2015) Label-free and enzyme-free homogeneous electrochemical biosensing strategy based on hybridization chain reaction: a facile, sensitive, and highly specific microRNA assay. Anal Chem 87:11368–11374

Huang WE, Stoecker K, Griffiths R, Newbold L, Daims H, Whiteley AS, Wagner M (2007) Raman-FISH: combining stable-isotope Raman spectroscopy and fluorescence *in situ* hybridization for the single cell analysis of identity and function. Environ Microbiol 9:1878–1889

Huang J, Wu Y, Chen Y, Zhu Z, Yang X, Yang CJ, Wang K, Tan W (2011) Pyrene-excimer probes based on the hybridization chain reaction for the detection of nucleic acids in complex biological fluids. Angew Chem Int Edit 50:401–404

Imachi H, Nobu MK, Nakahara N, Morono Y, Ogawara M, Takaki Y, Takano Y, Uematsu K, Ikuta T, Ito M, Matsui Y, Miyazaki M, Murata K, Saito Y, Sakai S, Song C, Tasumi E, Yamanaka Y, Yamaguchi T, Kamagata Y et al (2020) Isolation of an archaeon at the prokaryote-eukaryote interface. Nature 577:519–525

Ishii K, Mussmann M, MacGregor BJ, Amann R (2004) An improved fluorescence in situ hybridization protocol for the identification of bacteria and archaea in marine sediments. FEMS Microbiol Ecol 50:203–213

Jia LP, Zhao RN, Wang LJ, Ma RN, Zhang W, Shang L, Wang HS (2018) Aptamer based electrochemical assay for protein kinase activity by coupling hybridization chain reaction. Biosens Bioelectron 117:690–695

Kallmeyer J, Smith DC, Spivack AJ, D'Hondt S (2008) New cell extraction procedure applied to deep subsurface sediments. Limnol Oceanogr Methods 6:236–245

Krsek M, Wellington E (1999) Comparison of different methods for the isolation and purification of total community DNA from soil. J Microbiol Methods 39:1–16

Krukenberg V, Riedel D, Gruber-Vodicka HR, Buttigieg PL, Tegetmeyer HE, Boetius A, Wegener G (2018) Gene expression and ultrastructure of meso- and thermophilic methanotrophic consortia. Environ Microbiol 20:1651–1666

Kubota K (2013) CARD-FISH for environmental microorganisms: technical advancement and future applications. Microbes Environ 28:3–12

Kubota K, Ohashi A, Imachi H, Harada H (2006) Visualization of *mcr* mRNA in a methanogen by fluorescence in situ hybridization with an oligonucleotide probe and two-pass tyramide signal amplification (two-pass TSA-FISH). J Microbiol Meth 66:521–528

Manzini G, Barcellona ML, Avitabile M, Quadrifoglio F (1983) Interaction of diamidino-2-phenylindole (DAPI) with natural and synthetic nucleic acids. Nucleic Acids Res 11:8861–8876

Massie H, Samis H, Baird M (1972) The kinetics of degradation of DNA and RNA by H_2O_2. Biochem Biophys Acta 272:539–548

Matsubayashi M, Shimada Y, Li YY, Harada H, Kubota K (2017) Phylogenetic diversity and *in situ* detection of eukaryotes in anaerobic sludge digesters. PLoS ONE 12:e0172888

Miao P, Tang Y, Yin J (2015) MicroRNA detection based on analyte triggered nanoparticle localization on a tetrahedral DNA modified electrode followed by hybridization chain reaction dual amplification. Chem Commun 51:15629–15632

Moraru C, Lam P, Fuchs BM, Kuypers MM, Amann R (2010) GeneFISH–an in situ technique for linking gene presence and cell identity in environmental microorganisms. Environ Microbiol 12:3057–3073

Morono Y, Terada T, Masui N, Inagaki F (2009) Discriminative detection and enumeration of microbial life in marine subsurface sediments. ISME J 3:503–511

Morono Y, Terada T, Kallmeyer J, Inagaki F (2013) An improved cell separation technique for marine subsurface sediments: applications for high-throughput analysis using flow cytometry and cell sorting. Environ Microbiol 15:2841–2849

Morono Y, Kubota K, Tsukagoshi D, Terada T (2020) EDTA-FISH: a simple and effective approach to reduce non-specific adsorption of probes in fluorescence *in situ* hybridization (FISH) for environmental samples. Microbes Environ 35:3

Morris RM, Rappe MS, Connon SA, Vergin KL, Siebold WA, Carlson CA, Giovannoni SJ (2002) SAR11 clade dominates ocean surface bacterioplankton communities. Nature 420:806–810

Nikolakakis K, Lehnert E, McFall-Ngai MJ, Ruby EG (2015) Use of hybridization chain reaction-fluorescent *in situ* hybridization to track gene expression by both partners during initiation of symbiosis. Appl Environ Microbiol 81:4728–4735

Orcutt B, Meile C (2008) Constraints on mechanisms and rates of anaerobic oxidation of methane by microbial consortia: process-based modeling of ANME-2 archaea and sulfate reducing bacteria interactions. Biogeosciences 5:1587–1599

Orphan VJ, Turk KA, Green AM, House CH (2009) Patterns of ^{15}N assimilation and growth of methanotrophic ANME-2 archaea and sulfate-reducing bacteria within structured syntrophic consortia revealed by FISH-SIMS. Environ Microbiol 11:1777–1791

Pernthaler A, Preston CM, Pernthaler J, DeLong EF, Amann R (2002) Comparison of fluorescently labeled oligonucleotide and polynucleotide probes for the detection of pelagic marine bacteria and archaea. Appl Environ Microbiol 68:661–667

Royet D, Dempsey NM, Simonet P, Frénéa-Robin M (2018) A new magnetic cell fishing approach based on hybridization chain reaction: HCR-MISH. Sensor Actuat B Chem 273:126–132

Schindelin J, Rueden CT, Hiner MC, Eliceiri KW (2015) The ImageJ ecosystem: an open platform for biomedical image analysis. Mol Reprod Dev 82:518–529

Sepulveda LA, Xu H, Zhang J, Wang MY, Golding I (2016) Measurement of gene regulation in individual cells reveals rapid switching between promoter states. Science 351:1218–1222

Skinner SO, Sepulveda LA, Xu H, Golding I (2013) Measuring mRNA copy number in individual *Escherichia coli* cells using single-molecule fluorescent *in situ* hybridization. Nat Protoc 8:1100–1113

So LH, Ghosh A, Zong C, Sepulveda LA, Segev R, Golding I (2011) General properties of transcriptional time series in *Escherichia coli*. Nat Genet 43:554–560

Sunamura M, Maruyama A, Tsuji T, Kurane R (2003) Spectral imaging detection and counting of microbial cells in marine sediment. J Microbiol Methods 53:57–65

Taniguchi Y, Choi PJ, Li GW, Chen HY, Babu M, Hearn J, Emili A, Xie XS (2010) Quantifying *E. coli* proteome and transcriptome with single-molecule sensitivity in single cells. Science 329:533–538

Wilen BM, Onuki M, Hermansson M, Lumley D, Mino T (2008) Microbial community structure in activated sludge floc analysed by fluorescence in situ hybridization and its relation to floc stability. Water Res 42:2300–2308

Wu J, Li N, Yao Y, Tang D, Yang D, Ong'achwa Machuki J, Li J, Yu Y, Gao F (2018) DNA-stabilized silver nanoclusters for label-free fluorescence imaging of cell surface glycans and fluorescence guided photothermal therapy. Anal Chem 90:14368–14375

Yamaguchi T, Kubota K (2017) Visualization of microorganisms in bioprocesses. In: Purohit HJ, Kalia VC, Vaidya AN, Khardenavis

AA (eds) Optimization and applicability of bioprocesses. Springer Singapore, Singapore, pp 13–26

Yamaguchi T, Fuchs BM, Amann R, Kawakami S, Kubota K, Hatamoto M, Yamaguchi T (2015a) Rapid and sensitive identification of marine bacteria by an improved *in situ* DNA hybridization chain reaction (quickHCR-FISH). Syst Appl Microbiol 38:400–405

Yamaguchi T, Kawakami S, Hatamoto M, Imachi H, Takahashi M, Araki N, Yamaguchi T, Kubota K (2015b) In situ DNA-hybridization chain reaction (HCR): a facilitated in situ HCR system for the detection of environmental microorganisms. Environ Microbiol 17:2532–2541

Yang S, Kim S, Kim D-K, Jeon An H, Bae Son J, Hedén Gynnå A, Ki Lee N (2019) Transcription and translation contribute to gene locus relocation to the nucleoid periphery in *E. coli*. Nat Commun 10:5131

Zeng R, Zhang L, Su L, Luo Z, Zhou Q, Tang D (2019) Photoelectro-chemical bioanalysis of antibiotics on rGO-Bi2WO6-Au based on branched hybridization chain reaction. Biosens Bioelectron 133:100–106

Zhang B, Liu B, Tang D, Niessner R, Chen G, Knopp D (2012) DNA-based hybridization chain reaction for amplified bioelectronic signal and ultrasensitive detection of proteins. Anal Chem 84:5392–5399

Zhang K, Lv S, Zhou Q, Tang D (2020) CoOOH nanosheets-coated g-C3N4/CuInS2 nanohybrids for photoelectrochemical biosensor of carcinoembryonic antigen coupling hybridization chain reaction with etching reaction. Sensor Actuat B Chem 307:127631